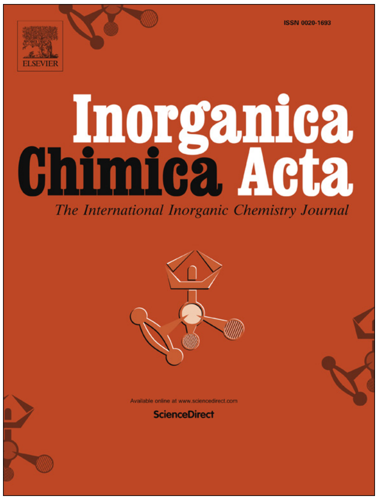

Synthesis, Structure, Magnetic Properties, and Catecholase-like Activity of a Phenoxo Bridged Dinuclear Cobalt(II) Complex

Shuranjan Sarkar, Hong-In Lee

PII:	S0020-1693(19)31599-3
DOI:	https://doi.org/10.1016/j.ica.2020.119437
Reference:	ICA 119437
To appear in:	*Inorganica Chimica Acta*
Received Date:	22 October 2019
Revised Date:	3 January 2020
Accepted Date:	10 January 2020

Please cite this article as: S. Sarkar, H-I. Lee, Synthesis, Structure, Magnetic Properties, and Catecholase-like Activity of a Phenoxo Bridged Dinuclear Cobalt(II) Complex, *Inorganica Chimica Acta* (2020), doi: https://doi.org/10.1016/j.ica.2020.119437

Synthesis, Structure, Magnetic Properties, and Catecholase-like Activity of a Phenoxo Bridged Dinuclear Cobalt(II) Complex

Shuranjan Sarkar[1] and Hong-In Lee*

Department of Chemistry and Green-Nano Materials Research Center, Kyungpook National University, Daegu 41566, Republic of Korea,

Abstract

A dinuclear cobalt complex Co_2L_2 (H_2L = *N,N'*-bis(salicylidene)-2,2'-ethylenedianiline) have been synthesized and characterized. X-ray crystallography found that Co_2L_2 contains a planar Co_2O_2 core where two Co(II) ions are bridged by two phenoxo ligands with Co-Co distance of 3.221 Å and the coordination geometry of each cobalt(II) ion is a distorted trigonal bipyramid. The magnetic susceptibility measurements revealed that both Co(II) ions are in low-spin (S = 1/2) states and two Co(II) spin centers are antiferromagnetically coupled with the exchange coupling constant of J = -45 cm^{-1}. Co_2L_2 showed catecholase-like activity when 3,5-di-*tert*-butylcatechol (3,5-H_2dtbc) was treated with Co_2L_2 in the presence of O_2 and NaOH with the turnover number of k_{cat} = 803 h^{-1}. Electron paramagnetic resonance (EPR) on the reaction mixture observed a key reaction intermediates, 3,5-di-*tert*-butyl-1,2-benzosemiquinonate anion radical (3,5-dtsq$^{\bullet-}$) bound to Co(III)-center. This is the first time observation of Co(III)-3,5-dtsq$^{\bullet-}$ intermediate during the oxidation of 3,5-H_2dtbc by a dicobalt(II/II) complex.

Key words: Cobalt complex, Dinuclear complex, Catecholase activity, Single crystal structure, Magnetic properties

1. Introduction

Catechol oxidase (catecholase) is a well-known type-3 copper enzyme, containing a dicopper center in its active site, which catalyzes the oxidation of a wide range of *o*-diphenyls to the corresponding *o*-quinones. These *o*-quinones can be autopolymerized to produce brown color polyphenolic pigments that protect tissue damage against pathogens.[1,2]. The crystal structures at the native *met* (Cu(II)-Cu(II)) state, the *deoxy* (Cu(I)-Cu(I)) state, and phenylthiourea inhibited state of the enzyme extracted from sweet potatoes (*Ipomoea batatas*) have been reported.[3] Based on the structural, spectroscopic, and theoretical investigations, several catalytic reaction pathways of the enzyme have been proposed. The reaction pathways could be classified into two categories in terms of the active oxidation states of the copper centers involved in the catalytic cycle; one in which both the *met* and *deoxy* states are active,[3,4] and the other in which only the *deoxy* state is active.[5,6]

---

* Corresponding author. Fax: +82 53 950 6331. *E-mail Address*: 1eehi@knu.ac.kr (H.-I. Lee).

[1] Present address: Chemistry Division, Bangladesh Jute Research Institute, Dhaka 1207, Bangladesh.

Functionality and reaction mechanisms of copper model complexes mimicking catechol oxidase have been extensively studied by investigating the oxidation of 3,5-di-*tert*-butylcatechol (3,5-H_2dtbc) to 3,5-di-*tert*-butyl-*o*-quinone (3,5-dtbq) in the presence of O_2.[7-32] In addition to the copper complexes, other metals, such as manganese[33-46], nickel[47-60], zinc[12,60-65], and cobalt[49,52,57,59,66-72] complexes have been also found to show catecholase activities. Among those complexes, searching the catalytic reaction pathways on the oxidation of 3,5-H_2dtbc by cobalt complexes is of interest because cobalt has three redox active states, I/II/III. Depending on both the oxidation states of the cobalt ions and the constitution, mono- or multicobalt, of the complexes, diversified reaction pathways have been proposed.[2,66,67,71-73] Until now, the suggested mechanistic pathways in general involve the formation of 3,5-di-*tert*-butyl-1,2-benzosemiquinonate anion radical (3,5-dtsq$^{\bullet-}$). However, the oxidation states of the metal ions are not clearly identified when the semiquinone anion radical is bound to the metal.

In this study, we have synthesized a dinuclear cobalt complex (Co_2L_2) derived from a tetradentate diphenolate ligand H_2L (H_2L = *N,N'*-bis(salicylidene)-2,2'-ethylenedianiline) to investigate the mechanistic details of the catecholase activity. (**Scheme 1**) Single crystal structure of the complex was determined to be a dicobalt(II) complex containing planar Co_2O_2 core where two cobalt(II) ions are bridged by two phenoxo ligands with Co(II)-Co(II) distance of 3.221 Å. The complex showed a high catecholase activity when it reacted with 3,5-H_2dtbc in the presence of O_2. Here, we explore the changes of the electronic and magnetic states during the oxidation of 3,5-H_2dtbc by Co_2L_2.

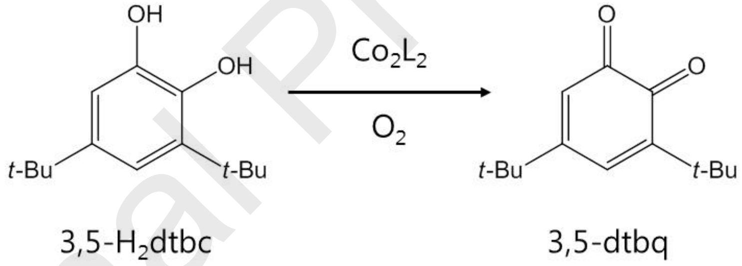

Scheme 1. Catalytic oxidation of 3,5-H_2dtbc by Co_2L_2

2. Experimental

2.1 Synthesis of N,N'-bis(salicylidene)-2,2'-ethylenedianiline (H_2L)

The ligand, H_2L, was prepared by following the previously reported literature method.[31,74] A solution of salicylaldehyde (0.75 g, 6.0 mmol) dissolved in 5 mL of dry toluene was added to a magnetically-stirred solution of 2,2'-ethylenedianiline (0.66 g, 3.0 mmol) dissolved in 20 mL of dry toluene. The mixture solution was refluxed for 2 hours. Yellow solid products were washed several times with methanol and dried under vacuum at ambient temperature. (**Scheme 2**) Yield: 90% (1.3 g), m.p. > 200^{o}C. The H_2L ligand was identified by FT-IR (**Fig. S1**) recorded from a KBr pellet and ^{1}H and ^{13}C NMR recorded in $CDCl_3$ at 25^{o}C showing identical features to the previously reported data.[74] (**Figs. S2** and **S3**) ^{1}H NMR (400 MHz, $CDCl_3$, 298 K): δ (ppm) = 13.22 (s, 2H, O*H*), 8.07 (s, 2H, NC*H*), 7.40-6.81 (m, 16H, Ar*H*), 3.04 (s, 4H, N(PhCH_2CH_2Ph)N). ^{13}C NMR (100 MHz, $CDCl_3$, 298 K): δ (ppm) = 162.92 (N*C*H), 161.41 (Ar*C*), 148.04 (Ar*C*), 135.50 (Ar*C*), 133.37 (Ar*C*), 132.73 (Ar*C*), 130.81 (Ar*C*), 127.64 (Ar*C*), 127.22 (ArC), 119.76 (Ar*C*), 119.35 (Ar*C*), 118.30 (Ar*C*H), 117.65 (Ar*C*), 33.50 (N(Ph*C*H_2*C*H_2Ph)N).

2.2 Synthesis of bis{N,N'-bis((salicylidene)-2,2'-ethylenedianiline)Cobalt(II)} (Co_2L_2)

A solution of $Co(ClO_4)_2\cdot 6H_2O$ (0.73 g, 2.0 mmol) dissolved in 10 mL of dry acetonitrile was added dropwise to a acetonitrile solution of H_2L (0.84 g, 2.0 mmol) and stirred 1 hour at room temperature. An aqueous solution of sodium hydroxide (0.16 g, 4.0 mmol) was added dropwise to the reaction mixture. The mixture solution was refluxed 1 hour and stirred overnight at ambient temperature. After the stirring, a wine-matte crystalline powder was collected by filtration. (**Scheme 2**) Yield: 88% (0.86 g), m.p. > 200°C. Elemental analysis calculated for $C_{56}H_{44}Co_2N_4O_4\cdot CH_3CN$ (mol. wt. = 995.89): C, 69.95%; H, 4.76%; N, 7.03%. Found: C, 69.39%; H, 4.74%; N 7.37 %. FAB MS analysis (*m*/*z*, +ion base): 955.30, $[Co_2L_2+H]^+$ 100 %. (**Fig. S4**) FT-IR (KBr disc., cm^{-1}, selected peaks): 1605 (ν_{immine}), 1585-1440 (ν_{benzene}). (**Fig. S5**). The powder was again dissolved in acetonitrile to be 1 x 10^{-3} M in a 10 mL vial. Suitable crystals for an X-ray analysis were obtained from the solution after two days.

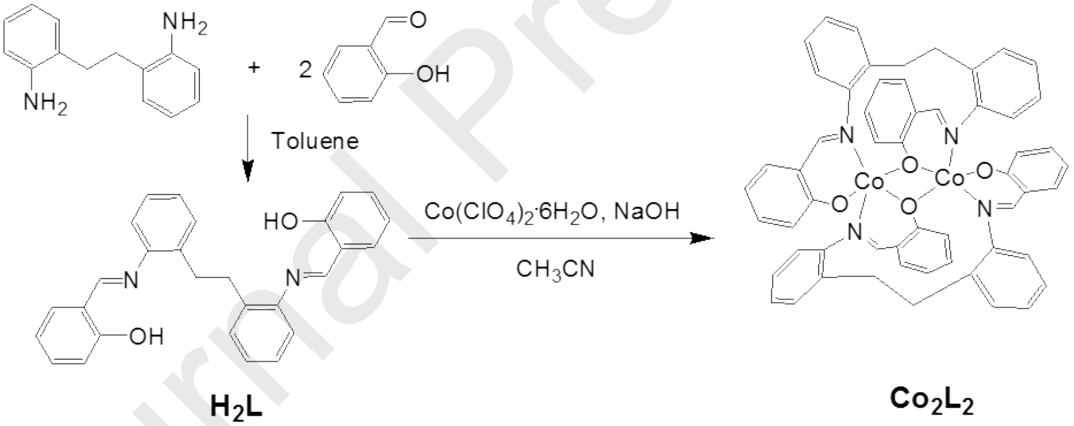

Scheme 2. Synthesis of Co_2L_2

2.3 X-ray Crystallography

A dark red crystal of Co_2L_2 was mounted on a glass fiber. X-ray data was collected on a Bruker SMART APEXII diffractometer equipped with graphite monochromated MoK_α radiation (λ = 0.71073 Å) at room temperature. (Korea Basic Research Institute, Seoul Western Center) The SMART and SAINT software package were used for data collection and integration.[75] SADABS was used for absorption correction.[76] The crystal structure was solved by the direct method and refined by full-matrix least-squares calculation with the SHELXTL software package.[77] All non-hydrogen atoms were refined anisotropically. The hydrogen atoms attached to C atoms were isotropically assigned with the isotropic displacement coefficients of $U(\mathrm{H}) = 1.2U$ (C), and their coordinates were allowed to ride on their respective atoms. A summary of the crystal and some crystallographic data are given in **Table 1**. CCDC-830840 contains the supplementary crystallographic data for this paper. These data can be obtained free of charge from The Cambridge Crystallographic Data Centre via www.ccdc.cam.ac.uk/data_request/cif.

Table 1. Crystal data and structure refinement for **Co_2L_2**

Empirical formula	$C_{56}H_{44}Co_2N_4O_4$
Formula weight	954.81
Temperature, K	296
Wavelength, Å	0.71073
Crystal system	Triclinic
Space group	$P\bar{1}$
a, Å	10.0029(5)
b, Å	14.8238(8)
c, Å	16.2529(8)
β, °	74.554(1)
Volume, Å^3	2262.0(2)
Z	2
Independent Reflections	11084 ($R_{\mathrm{int}} = 0.054$)
Goodness-of-fit on F^2	1.048
Final R indices $[I > 2\sigma(I)]^{a,b}$	$R_1 = 0.0679$, $wR_2 = 0.0915$
R indices (all data)	$R_1 = 0.1856$, $wR_2 = 0.1326$
Largest diff. peak and hole, e·Å^{-3}	0.628 and -0.689

$^aR_1 = \Sigma||F_0|-|F_c||/\Sigma|F_0|$, $^bwR_2 = [\Sigma w(F_0^2-F_c^2)^2/\Sigma wF_0^4]^{1/2}$

2.4 Physical measurements

NMR spectra were recorded on a Bruker Advance Digital 400-NMR spectrometer and chemical shifts were recorded in ppm units. The elemental analysis was performed using a Perkin-Elmer 2400 CHN analyzer. UV/Vis electronic spectra were recorded with a Scinco UV S-2100 spectrophotometer. Magnetic susceptibilities were measured in the applied magnetic field of 5000 Oe from 2 to 300 K on a Quantum Design MPMS superconducting quantum interference device (SQUID) magnetometer equipped with a 5.5 T magnet. Paramagnetic susceptibilities were calculated by subtracting diamagnetic effects from the observed magnetic susceptibilities using Pascal's constants. Fitting of magnetic susceptibility was performed using a home-made program written in MATLAB® software without considering anisotropic parameters. The program can be obtained upon requesting to the corresponding author. X-band (9 GHz) electron paramagnetic resonance (EPR) spectra were collected on a Jeol JES-TE300 ESR spectrometer using a 100 kHz field modulation. Low temperature EPR spectra were obtained using a Jeol ES-DVT3 variable temperature controller. The spectral simulations of EPR were performed using the program EasySpin.[78]

3. Results and Discussion

3.1 Synthesis and Structure

The ligand, H_2L, was prepared by following the previous method.[31,74] An acetonitrile solution of $Co(ClO_4)_2 \cdot 6H_2O$ was added dropwise to an acetonitrile solution of H_2L and stirred 1 hour. An aqueous solution of sodium hydroxide was added to the solution. The resulting solution was refluxed 1 hour and stirred overnight to give a wine matte crystalline powder. Suitable crystals of Co_2L_2 for X-ray analysis were obtained by recrystallization in acetonitrile.

Co_2L_2 was structurally characterized by a single crystal X-ray diffraction study. **Table 1** presents the crystal data. Co_2L_2 crystallized in a triclinic unit cell containing two dimeric entities. **Fig. 1** shows the molecular structure of Co_2L_2 together with the labeling scheme used. The structure can be viewed as a dicobalt(II) complex containing Co_2O_2 core where two cobalt(II) ions are bridged by two phenoxo ligands with Co(II)-Co(II) distance of 3.221 Å and Co(II)-$O_{bridging}$ bond lengths of 2.015(3) - 2.087(3) Å. The Co_2O_2 core is essentially planar with the maximum deviation of 0.125 Å from the least-squares plane. The Co_2O_2 core is similar to the situation found in other phenoxo-bridged dinuclear cobalt(II) complexes.[79-82] Each cobalt ion additionally coordinates to two imine nitrogens and a phenoxo ligand to complete a distorted trigonal bipyramidal coordination geometry ($\tau = 0.83$ for Co1 and 0.63 for Co2)[83] whose apical positions are occupied by the terminal phenoxo oxygen and one of the bridging phenoxo oxygens. The Co(II)-$O_{terminal}$ bond lengths of 1.934(4) - 1.938(3) Å are shorter than the Co(II)-$O_{bridging}$ bond lengths. The Co(II)-N_{imine} bond lengths of 2.052(4) - 2.114(4) Å are in agreement with those found in other pentacoordinated Co(II) complexes.[79-82,84] Selected bond lengths and angles with estimated standard deviations are listed in **Table 2**.

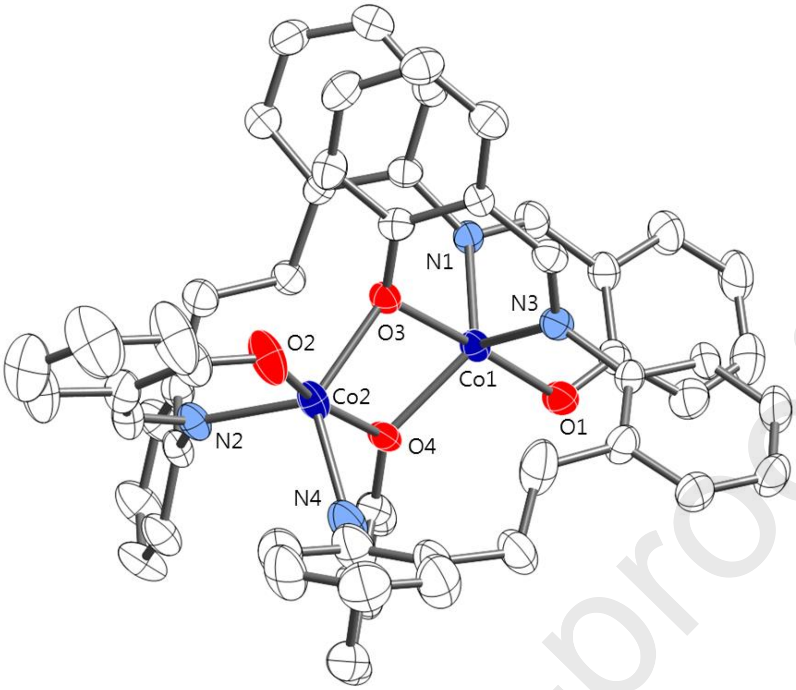

Fig. 1. Crystal structure of of Co_2L_2 with 33% probability thermal ellipsoids. Hydrogen atoms have been omitted for clarity.

Table 2. Selected bond lengths and angles for $\mathbf{Co_2L_2}$.

	Bond lengths (Å)		
Co1-N1	2.073(4)	Co2-N2	2.052(4)
Co1-N3	2.114(4)	Co2-N4	2.103(5)
Co1-O1	1.938(3)	Co2-O2	1.934(4)
Co1-O3	2.087(3)	Co2-O3	2.015(3)
Co1-O4	2.015(3)	Co2-O4	2.084(3)
	Bond angles (°)		
N1-Co1-N3	109.61(14)	N2-Co2-N4	101.88(17)
N1-Co1-O1	92.93(15)	N2-Co2-O2	92.63(16)
N1-Co1-O3	91.86(14)	N2-Co2-O3	123.49(14)
N1-Co1-O4	125.44(13)	N2-Co2-O4	97.96(15)
N3-Co1-O1	95.96(15)	N4-Co2-O2	98.08(19)
N3-Co1-O3	81.55(14)	N4-Co2-O3	131.10(16)
N3-Co1-O4	119.81(13)	N4-Co2-O4	82.33(17)
O1-Co1-O3	175.13(13)	O2-Co2-O3	97.12(14)
O1-Co1-O4	103.04(13)	O2-Co2-O4	169.10(14)
O3-Co1-O4	74.82(12)	O3-Co2-O4	74.86(11)

3.2 Catecholase activity

Initial tests of the catalytic activities of Co_2L_2 showed a catecholase activity of the complex. Indepth investigation for the catecholase activity was performed by treating an acetronitrile solution of Co_2L_2 with 3,5-di-*tert*-butylcatechol (3,5-H_2dtbc) in air. The oxidized product, 3,5-di-*tert*-butyl-*o*-quinone (3,5-dtbq), has a strong absorption at λ_{max} = 400 nm (ε = 1,900 $M^{-1}cm^{-1}$), which allows the activity and reaction rate, respectively, to be determined.[16,31,32] **Fig. 2** shows the change of UV/Vis spectra at room temperature upon adding 3,5-H_2dtbc (3.75 x 10^{-4} M, 1.13 x 10^{-6} mol) into the Co_2L_2 solution (2.5 x 10^{-5} M, 7.5 x 10^{-8} mol) containing 4 equivalents of aqueous sodium hydroxide. As observed in the figure, the quinone band at 400 nm increases over time on top of the broad LMCT band of Co_2L_2 at 365 nm. The intensity was saturated at 450 sec after the reaction was initiated. The amount of 3,5-dtbq generated by the reaction was determined to be 8.53 x 10^{-7} mol which is much more than the amount of Co_2L_2, indicating the catalytic activity of Co_2L_2.

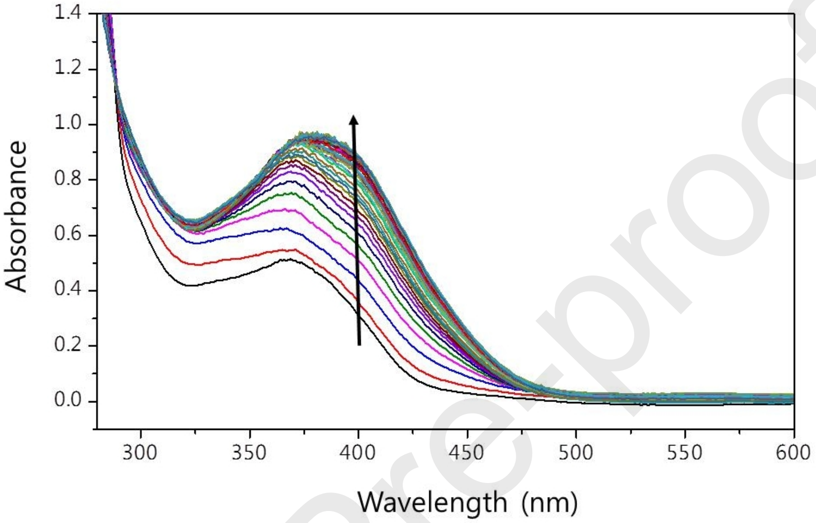

Fig. 2. Change of UV-VIS absorption spectra of Co_2L_2 + 3.5-H_2dtbc + NaOH in acetonitrile. The reaction was initiated by adding 3,5-H_2dtbc solution (3.75 x 10^{-4} M, 1.13 x 10^{-6} mol) into Co_2L_2 (2.5 x 10^{-5} M, 7.5 x 10^{-8} mol) solution containing 3.0 x 10^{-7} mol NaOH. Each spectrum was obtained every 10 second up to 450 seconds after mixing. Arrow denotes the increase of 3.5-dtbq absorption band.

The kinetics of the oxidation of 3,5-H_2dtbc by Co_2L_2 was investigated using the initial rate method. **Fig. 3** shows the concentration changes of the reaction product, 3,5-dtbq, *vs*. the reaction time, and the corresponding Michaelis-Menten and Lineweaver-Burk plots, respectively, when 2.5 x 10^{-5} M Co_2L_2 solution was mixed with 1-25 equivalents of 3,5-H_2dtbc in basic condition. From the analysis, the kinetic parameters of $V_{\max}$ = 5.57 x 10^{-6} Ms^{-1}, K_M = 1.93 x 10^{-4} M, k_{cat} = 0.223 s^{-1}, and k_{cat}/K_M = 1155 $M^{-1}s^{-1}$ were obtained. The blank tests found that the reaction rate of the Co_2L_2-catalyzed reaction was more than one order of magnitude faster than those of the reactions with the free ligand, H_2L, or cobalt salt in the absence or presence of NaOH. The reaction rate of the catecholase activity of Co_2L_2 in the absence of NaOH was significantly slower than **Fig.3**. The reaction rate was dependent on the concentration of NaOH which was used for enhancing the deprotonation of 3.5-H_2dtbc in the aprotic solvent.[85-88]

Previous studies on catecholase activities of cobalt model complexes have showed wide range of k_{cat} values from less than 10 h^{-1} to 24000 h^{-1}. (**Table 3**)[2,66-72,89,90] k_{cat} value of 803 h^{-1} (= 0.223 s^{-1}) observed from Co_2L_2 is comparable to those with moderate to high catecholase activities. **Fig. S6** displays the concentrations of 3,5-dtbq at 450 sec after the reactions started according to the initial concentrations of 3,5-H_2dtbc. The plot of [3,5-dtbq] *vs* [3,5-H_2dtbc]$_0$ is well explained by a linear line with the slope of 0.79, indicating that about 79% of 3,5-H_2dtbc were converted to 3,5-dtbq. This is in good agreement with the conversion ratio of oxidation of 3,5-H_2dtbc by our previous copper complex.[32]

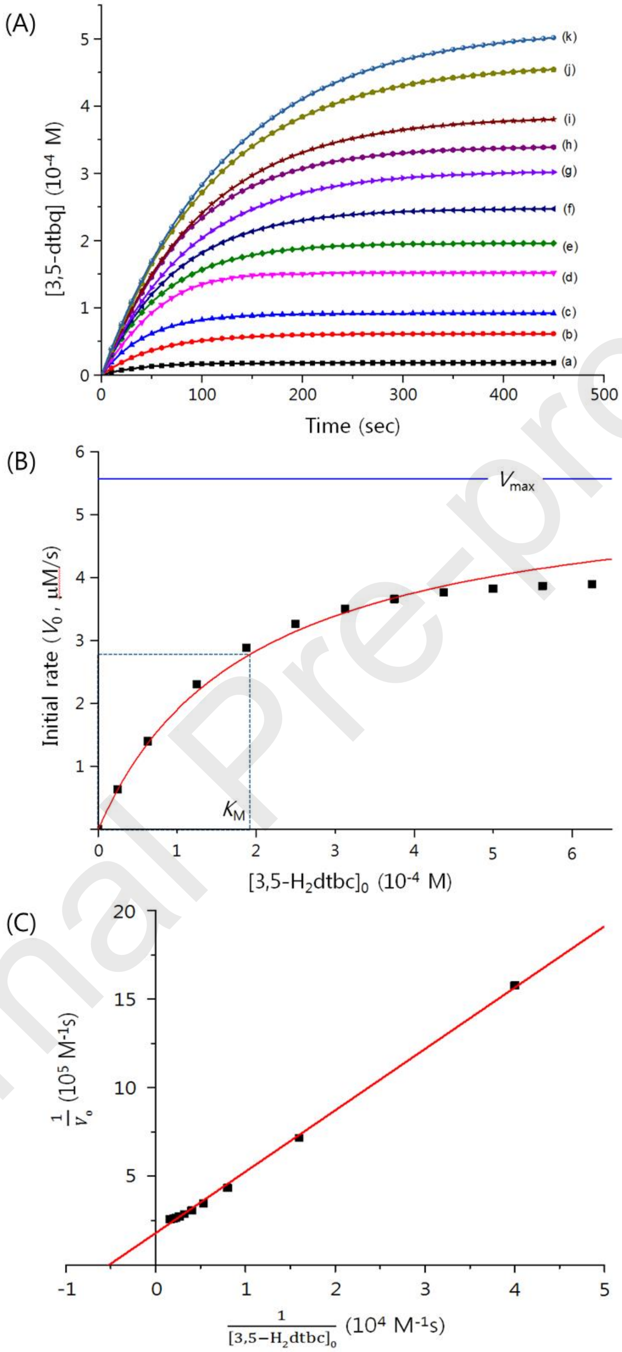

Fig. 3. Kinetic study of the catalytic oxidation of 3,5-H_2dtbc by Co_2L_2. $[Co_2L_2]_0$ = 2.5 x 10^{-5} M. $[NaOH]_0$ = 1.0 x 10^{-4} M. (A) [3.5-H_2dtbc] *vs*. time. Concentrations of 3,5-dtbq were calculated from the absorbances at λ_{max} = 400 nm (ε = 1,900 $M^{-1}cm^{-1}$). [3.5-H_2dtbc]$_0$ = (a) 2.5 x 10^{-5} M, (b) 6.25 x 10^{-5} M, (c) 1.25 x 10^{-4} M, (d) 1.875 x 10^{-4} M, (e) 2.5 x 10^{-4} M, (f) 3.125 x 10^{-4} M, (g) 3.75 x 10^{-3} M, (h) 4.375 x 10^{-4} M, (i) 5 x 10^{-4} M, (j) 5.625 x 10^{-4}, and (k) 6.25 x 10^{-4} M. (B) Corresponding Michaelis-Menten plot and (C) Lineweaver-Burk plot.

Table 3. Kinetic parameters for the catalytic oxidation of 3,5-H_2dtbc by cobalt complexes.

Complex	V_{max} (Ms^{-1})	k_{cat} (s^{-1})	K_M (M)	k_{cat} / K_M ($M^{-1}s^{-1}$)	Ref.
Co_2L_2	5.57×10^{-6}	2.23×10^{-1}	1.93×10^{-4}	1160	This work
$Co(Hdmg)_2(Ph_3P)_2$		$7.4\ (3.7) \times 10^{-2}$			[66,67]
$[Co_2(L^1)]^+$		8.5×10^{-3}			[89]
$[Co_2(L^2)]^+$		9.1×10^{-3}			[89]
$[Co_2(EGTB)Cl_2]^+$	1.95×10^{-7}	1.95×10^{-3}	2.77×10^{-3}	0.704	[68]
$[Co_2(L^1H)(H_2O)_2(OAc)_2]^{+2}$	1.24×10^{-4}	1.24×10^{-1}	2.45×10^{-3}	50.6	[69]
$[Co_2(L^2)(H_2O)_2(OAc)_2]^+$	1.28×10^{-5}	1.28×10^{-2}	1.78×10^{-3}	7.19	[69]
$[Co_2(L^3)(H_2O)_2(OAc)_2]^+$	1.19×10^{-5}	1.19×10^{-2}	2.39×10^{-3}	4.98	[69]
$[Co_2(HL^1)_2(H_2O)(HOCH_2CH_3)]^+$	5.95×10^{-4}	5.95	8.82×10^{-3}	675	[70]
$Co_3(H_2L^2)_2(L^2)Cl_2$	6.76×10^{-4}	6.76	8.97×10^{-3}	754	[70]
$Co(L)(N_3)_2(H_3O^+)$	6.97×10^{-6}	2.78×10^{-3}	1.26×10^{-3}	22.1	[90]
$Co(L)(NCS)(H_2O)$	7.80×10^{-8}	3.11×10^{-3}	1.24×10^{-3}	2.51	[90]
$Co_2(H_2L)_2(OAc)_2$	2.22×10^{-7}	2.19×10^{-2}	8.7×10^{-3}	2.52	[71]
cis-$[Co_3L_2(MeOH)_2(N_3)_2(\mu_{1,1}\text{-}N_3)_2]$	1.97×10^{-6}	3.94×10^{-2}	1.89×10^{-3}	20.9	[72]
trans-$[Co_3L_2(H_2O)_2(N_3)_2(\mu_{1,1}\text{-}N_3)_2]$	1.20×10^{-6}	2.36×10^{-2}	1.44×10^{-3}	16.4	[72]
$Co_3L^R{}_2(N_3)_3(\mu_{1,3}\text{-}N_3)_2$	1.38×10^{-6}	2.75×10^{-2}	1.65×10^{-3}	16.7	[72]

3.3 Magnetic properties

The magnetic susceptibility of Co_2L_2 was measured over the temperature range of 2 K – 300 K in the applied magnetic field of 5000 Oe. As shown in **Fig. 4(A)**, the molar magnetic susceptibility (χ_m) decreases as temperature increases with maximum at near 34 K, indicating an antiferromagnetic coupling between the spin centers. Sharp increase of χ_m at very low temperature may be due paramagnetic impurities. The antiferromagnetic nature of Co_2L_2 is also observed from the $\chi_m T$ *vs*. T plot in which $\chi_m T$ decreases as temperature decreases. (**Fig. 4(B)**) $\chi_m T$ at room temperature is calculated to be 1.12 cm^3/mol which gives the magnetic moment of 2.12 μ_B per Co(II) ion. Co(II) ion, with d^7 electron configuration, can have either $S = 1/2$ (low-spin) or $S = 3/2$ (high-spin) spin state, of which the theoretical spin-only magnetic moment is 1.73 μ_B or 3.87 μ_B, respectively. This clearly demonstrates that both the Co(II) ions of Co_2L_2 are in low-spin ($S = 1/2$) states.

To estimate the magnitude of the exchange coupling between two Co(II) centers, χ_m was fitted with the following equation,[91,92]

$$\chi_m = \chi_0 + \frac{C_{imp}}{T - \theta_{imp}} + \frac{Ng^2\mu_B^2}{kT[3 + e^{-\frac{J}{kT}}]} \qquad (1)$$

where χ_o and $C_{imp}/(T - \theta_{imp})$ are the temperature independent and dependent magnetic susceptibilities of paramagnetic impurities, respectively. The best fit parameters are $\chi_o = 4.4 \times 10^{-4}$ cm^3/mol, $C_{imp} = 0.23$ cm^3K/mol, $\theta_{imp} = -14$ K, and J = -45 cm^{-1} with fixed g = 2.0, indicating strong antiferromagnetic coupling between two spin centers.

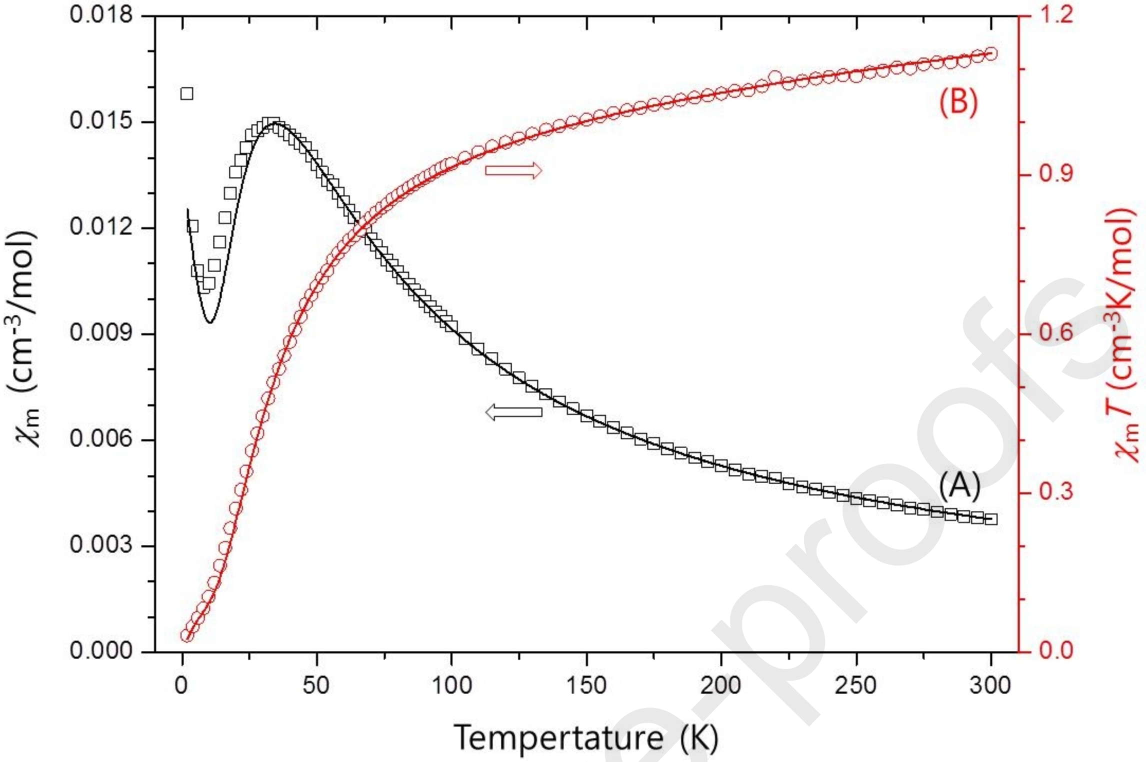

Fig. 4. Plots of (A) molar magnetic susceptibility (χ_m, black square) *vs* T and (B) $\chi_m T$ (red circle) *vs* T of Co_2L_2. Solid lines are the fit using the equation (1). *Fitting parameters*: χ_o = 4.4 x 10^{-4} cm^3/mol, C_{imp} = 0.23 cm^{3}K/mol, θ_{imp} = -14 K, J = -45 cm^{-1}, and g = 2.0.

3. 4 Electron Paramagnetic Resonance

EPR (electron paramagnetic resonance) is useful for monitoring the changes of the metal oxidation states and radical intermediates during the catalytic reaction. To observed such changes, EPR spectra were recorded after adding 3,5-H_2dtbc (1.3 x 10^{-2} M, 4.0 x 10^{-5} mol) into the Co_2L_2 solution (6.7 x 10^{-4} M, 2.0 x 10^{-6} mol) containing 4 equivalents of aqueous sodium hydroxide. **Fig. 5(A)** displays EPR spectra obtained from the frozen acetonitrile solution of the reaction mixture at 110 K. EPR spectrum at 0 sec, which was obtained from the Co_2L_2 solution containing sodium hydroxide, did not give any detectable EPR intensity due to strong antiferromagnetic coupling of two low-spin Co(II) ions. After adding 3,5-H_2dtbc, EPR signal gradually increases over the reaction time. The observed EPR spectra could be well simulated with $\boldsymbol{g}$ = [2.003 2.003 2.001] and $\boldsymbol{A}_{Co}$ = [16.5 16.5 47.6] MHz. EPR spectrum obtained from the reaction-mixture solution at room temperature shows 16 lines or 8 doublets. (**Fig. 5(B)**) This splitting is due to the nuclear hyperfine couplings of ^{59}Co (I = $^7/_2$) and ^{1}H (I = $^1/_2$), which is confirmed by the numerical simulation with g_{iso}= 2.0023 and the isotropic nuclear hyperfine coupling constants of $A_{Co,iso}$ = 26.8 MHz and $A_{H,iso}$ = 9.2 MHz. Calculated g_{iso} (= 2.002) and $A_{Co,iso}$ (= 26.9 MHz) values extracted from the simulation of the frozen solution EPR (**Fig. 5(A)**) are essentially the same as those obtained from the solution EPR (**Fig. 5(B)**) at room temperature, indicating that both the EPR spectra in **Figs. 5(A)** and **5(B)** are arising from the same chemical species. In the frozen solution EPR, ^{1}H hyperfine coupling is not resolved under the inhomogeneously broadened EPR line caused by g- and $\boldsymbol{A}_{\mathrm{Co}}$-anisotropies.

Since the EPR measurements at both room temperature and 110 K detected the ^{59}Co hyperfine coupling, the signal can be assigned to either low-spin Co(II) (d^7, S = 1/2) or a radical species coupled to low-spin Co(III) (d^6, S = 0). EPR of low-spin Co(II) shows wide range of g- and A_{Co}-values depending on the coordination geometries and ligand atoms.[93-99] In general, g-anisotropy and A_{iso} of low-spin Co(II) are bigger than those observed in this work, suggesting that a radical species coupled to low-spin Co(III) gives rise to EPR of **Fig. 5**. Previously, EPR of low-spin Co(III)-3,5-dtsq$^{\bullet-}$ (=3,5-di-*tert*-butyl-1,2-benzosemiquinonate anion radical) complex has been reported with the ring ^{1}H hyperfine of 3.3-3.5 G and the ^{59}Co hyperfine of 10-11 G which are close to our results.[66,67,73,100] These confirms the EPR spectra obtained during the catalytic oxidation of 3,5-H$_2$dtbc by Co$_2$L$_2$ are arising from an intermediate containing low-spin Co(III)-3,5-dtsq$^{\bullet-}$. Free 3,5-dtsq$^{\bullet-}$ radical in solution has been often detected by EPR.[30,32,101] However, such signal has not been observed during the oxidation of 3,5-H$_2$dtbc by Co$_2$L$_2$.

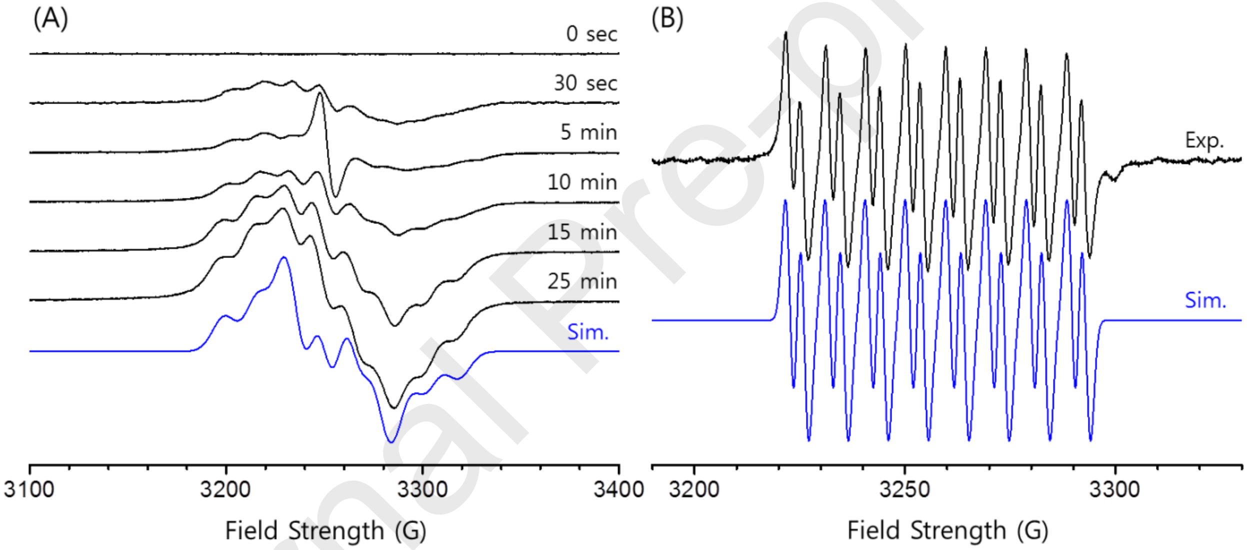

Fig. 5. (A) EPR spectra obtained from the frozen CH$_3$CN solution of Co$_2$L$_2$ + NaOH + 3,5-H$_2$dtbc and a corresponding numerical simulation, and (B) EPR spectra obtained from the CH$_3$CN solution of Co$_2$L$_2$ + NaOH + 3,5-H$_2$dtbc and a corresponding numerical simulation (5 min after mixing). *Experimental conditions*: microwave frequency, 9.13 GHz; microwave power, 1 mW; modulation amplitude, 0.5 G; modulation frequency, 100 kHz; time constant, 0.3 sec; scan speed, 125 G/min; temperature, 110 K (for A) and 298 K (for B); [Co$_2$L$_2$]$_0$ = 6.7 x 10^{-4} M, [NaOH]$_0$ = 2.7 x 10^{-3} M; and [3.5-H$_2$dtbc]$_0$ = 1.3 x 10^{-2} M. *Simulation parameters*: (A) $\boldsymbol{g}$ = [2.003 2.003 2.001]; $\boldsymbol{A}_{\mathrm{Co}}$ = [16.5 16.5 47.6] MHz, and (B) g_{iso} = 2.0023; $A_{\mathrm{H,iso}}$ = 9.2 MHz; $A_{\mathrm{Co,iso}}$ = 26.8 MHz.

3.5 Implication for Mechanistic Pathway

EPR measurements found a key reaction intermediate, low-spin Co(III)-3,5-dtsq$^{\bullet-}$, during the oxidation of 3,5-H$_2$dtbc by Co$_2$L$_2$ in the presence of O$_2$ (**Fig. 5**). Though the generation of Co(III)-3,5-dtsq$^{\bullet-}$ intermediates during the oxidation of 3,5-H$_2$dtbc by monomeric Co(II) complexes has been suggested,[66,67,89] the observation of the intermediate species from dicobalt(II/II) complexes has not been reported. Previously, the oxidation of 3,5-H_2dtbc by dicobalt complexes involved either with Co(II)-3,5-dtsq$^{\bullet-}$ or without 3,5-dtsq$^{\bullet-}$ intermediate depending on both the binding modes of 3,5-H_2dtbc, monodentate or bridging bidentate, and the oxidation states of the cobalt centers.[71,102] Observation of Co(III)-3,5-dtsq$^{\bullet-}$ in the catecholase activity of Co_2L_2 is likely to implying that only one cobalt site of Co_2L_2 is active for the catalysis. However, a fragmentation during the reaction cannot be ruled out.[103] More detailed investigation including the dependence of OH^- is currently underway for setting up a mechanistic pathway.

The oxidation product, 3,5-dtbq, has been often generated via disproportionation or air oxidation of free 3,5-dtsq$^{\bullet-}$ radical in solution which has been easily detected by EPR.[30,32] But such a signal was not observed during the oxidation of 3,5-H_2dtbc by Co_2L_2 indicating that 3,5-dtsq$^{\bullet-}$ was not freed from the intermediate complexes. There have been numerous reports showing valence tautomerism in cobalt and *o*-quinone complexes.[66,67,73,104-107] Therefore it is most probable that the last part of the mechanistic pathway is a valence tautomerization between Co(III)-center and 3,5-dtsq$^{\bullet-}$ in which Co(III)L-3,5-dtsq$^{\bullet-}$ is in equilibrium with Co(II)L + 3,5-dtbq.

4. Conclusion

In summary, we have taken a compartmental ligand, H_2L, containing N_2O_2 chelate groups to build dicobalt(II) complex, Co_2L_2. The complex contains a planar Co_2O_2 core where two cobalt(II) ions are bridged by two phenoxo ligands with Co(II)-Co(II) distance of 3.221 Å. The magnetic susceptibility measurements of Co_2L_2 found that both Co(II) ions are in low-spin (S = 1/2) configuration and two Co(II) spin centers are antiferromagnetically coupled with the exchange coupling constant of J = -45 cm^{-1}. Co_2L_2 showed catecholase-like activity when 3,5-di-*tert*-butylcatechol (3,5-H_2dtbc) was treated with Co_2L_2 in the presence of O_2 and NaOH. Kinetic investigation for the oxidation of 3,5-H_2dtbc to 3,5-di-*tert*-butyl-*o*-quinone (3,5-dtbq) by Co_2L_2 in acetonitrile found the turnover number of k_{cat} = 803 h^{-1}, which is relatively high catecholase activity in Co complexes. EPR of the reaction mixtures observed the reaction intermediate of a low-spin Co(III) complex containing 3,5-dtsq$^{\bullet-}$ ligand. This is the first time observation of of Co(III)-3,5-dtsq$^{\bullet-}$ intermediate during the oxidation of 3,5-H_2dtbc by a dicobalt(II/II) complex. The oxidation product, 3,5-dtbq, was probably generated via a valence tautomerization between Co(III)-center and 3,5-dtsq$^{\bullet-}$.

Declaration of Competing Interest

The authors declare that they have no known competing financial interests or personal relationships that could have appeared to influence the work reported in this paper.

Acknowledgements

This work was supported by the National Research Foundation of Korea Grant funded by the Korean Government (NRF-2018R1D1A1B07051018).

Appendix A: Crystallographic Data

CCDC-830840 contains the supplementary crystallographic data for this paper. These data can be obtained free of charge from The Cambridge Crystallographic Data Centre via www.ccdc.cam.ac.uk/data_request/cif.

Appendix B: Supplementary Data

Supplementary data to this article can be found online at ……

References

[1] I.A. Koval, P. Gamez, C. Belle, K. Selmeczi, J. Reedijk, Chem. Soc. Rev. 35 (2006) 814-840.
[2] S.K. Dey, A. Mukherjee, Coord. Chem. Rev. 310 (2016) 80-115.
[3] T. Klabunde, C. Eicken, J.C. Sacchettini, B. Krebs, Nat. Struct. Biol. 5 (1998) 1084-1090.
[4] E. Solomon, U. Sundaram, T. Machonkin, Chem. Rev. 96 (1996) 2563-2605.
[5] P.E.M. Siegbahn, J. Biol. Inorg Chem. 9 (2004) 577-590.
[6] M. Guell, P.E.M. Siegbahn, J. Biol. Inorg Chem. 12 (2007) 1251-1264.
[7] E. Monzani, G. Battaini, A. Perotti, L. Casella, M. Gullotti, L. Santagostini, G. Nardin, L. Randaccio, S. Geremia, P. Zanello, G. Opromolla, Inorg. Chem. 38 (1999) 5359-5369.
[8] C.H. Kao, H.H. Wei, Y.H. Liu, G.H. Lee, Y. Wang, C.J. Lee, J. Inorg. Biochem. 84 (2001) 171-178.
[9] C. Belle, C. Beguin, I. Gautier-Luneau, S. Hamman, C. Philouze, J.L. Pierre, F. Thomas, S. Torelli, Inorg. Chem. 41 (2002) 479-491.
[10] G. Battaini, E. Monzani, L. Casella, L. Santagostini, R. Pagliarin, J. Biol. Inorg Chem. 5 (2000) 262-268.
[11] R. Wegner, M. Gottschaldt, W. Poppitz, E.G. Jager, D. Klemm, J. Mol. Catal. A-Chem. 201 (2003) 93-118.
[12] J. Kaizer, R. Csonka, G. Speier, M. Giorgi, M. Reglier, J. Mol. Catal. A-Chem. 235 (2005) 81-87.
[13] M. Kodera, T. Kawata, K. Kano, Y. Tachi, S. Itoh, S. Kojo, Bull. Chem. Soc. Jpn. 76 (2003) 1957-1964.
[14] A. Neves, L.M. Rossi, A.J. Bortoluzzi, B. Szpoganicz, C. Wiezbicki, E. Schwingel, Inorg. Chem. 41 (2002) 1788-1794.
[15] J. Mukherjee, R. Mukherjee, Inorg. Chim. Acta. 337 (2002) 429-438.
[16] O. Seneque, M. Campion, N. Douziech, M. Giorgi, E. Riviere, Y. Journaux, Y. Le Mest, O. Eur. J. Inorg. Chem. (2002) 2007-2014.
[17] M. Merkel, N. Moller, M. Piacenza, S. Grimme, A. Rompel, B. Krebs, Chem. Eur. J. 11 (2005) 1201-1209.
[18] X. Wang, J. Ding, J.J. Vittal, Inorg. Chim. Acta. 359 (2006) 3481-3490.
[19] B. Sreenivasulu, F. Zhao, S. Gao, J.J. Vittal, Eur. J. Inorg. Chem. (2006) 2656-2670.
[20] R.A. Peralta, A. Neves, A.J. Bortoluzzi, A. dos Anjos, F.R. Xavier, B. Szpoganicz, H. Terenzi, M.C.B. de Oliveira, E. Castellano, G.R. Friedermann, A.S. Mangrich, M.A. Novak, J. Inorg. Biochem. 100 (2006) 992-1004.
[21] J. Ackermann, S. Buchler, F. Meyer, CR Chim. 10 (2007) 421-432.
[22] I.A. Koval, K. Sehmeczi, C. Belle, C. Philouze, E. Saint-Aman, I. Gautier-Luneau, A.M. Schuitema, M. van Vliet, P. Gamez, O. Roubeau, M. Lueken, B. Krebs, M. Lutz, A.L. Spek, J. Pierre, J. Reedijk, Chem. Eur. J. 12 (2006) 6138-6150.

[23] W.A. Alves, S.A. de Almeida, M.V. de Almeida, A. Paduan, C.C. Becerra, A.M.D. Ferreira, J. Mol. Catal. A-Chem. 198 (2003) 63-75.
[24] L. Gasque, V.M. Ugalde-Saldivar, I. Membrillo, J. Olguin, E. Mijangos, S. Bernes, I. Gonzalez, J. Inorg. Biochem. 102 (2008) 1227-1235.
[25] L. Gonzalez-Sebastian, V. Manuel Ugalde-Saldivar, E. Mijangos, M. Rosa Mendoza-Quijano, L. Ortiz-Frade, L. Gasque, J. Inorg. Biochem. 104 (2010) 1112-1118.
[26] E. Mijangos, J. Reedijk, L. Gasque, Dalton Trans. (2008) 1857-1863.
[27] R. Marion, M. Zaarour, N.A. Qachachi, N.M. Saleh, F. Justaud, D. Floner, O. Lavastre, F. Geneste, J. Inorg. Biochem. 105 (2011) 1391-1397.
[28] M.K. Panda, M.M. Shaikh, R.J. Butcher, P. Ghosh, Inorg. Chim. Acta. 372 (2011) 145-151.
[29] S. Majumder, S. Sarkar, S. Sasmal, E.C. Sanudo, S. Mohanta, Inorg. Chem. 50 (2011) 7540-7554.
[30] M. Rosa Mendoza-Quijano, G. Ferrer-Sueta, M. Flores-Alamo, N. Aliaga-Alcalde, V. Gomez-Vidales, V.M. Ugalde-Saldivar, L. Gasque, Dalton Trans. 41 (2012) 4985-4997.
[31] S. Sarkar, W.R. Lee, C.S. Hong, H. Lee, Bull. Kor. Chem. Soc. 34 (2013) 2731-2736.
[32] S. Sarkar, A. Sim, S. Kim, H. Lee, J. Mol. Catal. Chem. 410 (2015) 149-159.
[33] M. Ashafaq, M. Raizada, M. Khalid, M. Shahid, M. Ahmad, Z.A. Siddiqi, J. Coord. Chem. 71 (2018) 2118-2145.
[34] K.S. Banu, T. Chattopadhyay, A. Banerjee, M. Mukherjee, S. Bhattacharya, G.K. Patra, E. Zangrando, D. Das, Dalton Trans. (2009) 8755-8764.
[35] P. Chakraborty, I. Majumder, K.S. Banu, B. Ghosh, H. Kara, E. Zangrando, D. Das, Dalton Trans. 45 (2016) 742-752.
[36] J. Kaizer, R. Csonka, G. Barath, G. Speier, Transit. Metal Chem. 32 (2007) 1047-1050.
[37] J. Kaizer, G. Barath, R. Csonka, G. Speier, L. Korecz, A. Rockenbauer, L. Parkanyi, J. Inorg. Biochem. 102 (2008) 773-780.
[38] P. Kar, Y. Ida, T. Kanetomo, M.G.B. Drew, T. Ishida, A. Ghosh, Dalton Trans. 44 (2015) 9795-9804.
[39] S.C. Kumar, A.K. Ghosh, J. Chen, R. Ghosh, Inorg. Chim. Acta. 464 (2017) 49-54.
[40] P. Maiti, T. Ghosh, A. Banerjee, A. Banerjee, S. Bhattacharya, E. Suresh, D. Das, Transit. Met. Chem. 36 (2011) 195-199.
[41] M. Mitra, A.K. Maji, B.K. Ghosh, G. Kaur, A.R. Choudhury, C. Lin, J. Ribas, R. Ghosh, Polyhedron. 61 (2013) 15-19.
[42] D. Mondal, M.C. Majee, Inorg. Chim. Acta. 465 (2017) 70-77.
[43] S. Mukherjee, T. Weyhermuller, E. Bothe, K. Wieghardt, P. Chaudhuri, Dalton Trans. (2004) 3842-3853.
[44] S. Sengupta, B.N. Mongal, S. Das, T.K. Panda, T.K. Mandal, M. Fleck, S.K. Chattopadhyay, S. Naskar, J. Coord. Chem. 71 (2018) 1214-1233.
[45] P. Seth, M.G.B. Drew, A. Ghosh, J. Mol. Catal. A-Chem. 365 (2012) 154-161.
[46] P. Seth, A. Ghosh, RSC Adv. 3 (2013) 3717-3725.
[47] P.K. Basu, M. Mitra, A. Ghosh, L. Thander, C. Lin, R. Ghosh, J. Chem. Sci. 126 (2014) 1635-1640.
[48] A. Biswas, L.K. Das, M.G.B. Drew, G. Aromi, P. Gamez, A. Ghosht, Inorg. Chem. 51 (2012) 7993-8001.
[49] P. Chakraborty, S. Majumder, A. Jana, S. Mohanta, Inorg. Chim. Acta. 410 (2014) 65-75.
[50] L.K. Das, A. Biswas, J.S. Kinyon, N.S. Dalal, H. Zhou, A. Ghosh, Inorg. Chem. 52 (2013) 11744-11757.
[51] M. Das, R. Nasani, M. Saha, S.M. Mobin, S. Mukhopadhyay, Dalton Trans. 44 (2015) 2299-2310.
[52] A.K. Ghosh, M. Mitra, A. Fathima, H. Yadav, A.R. Choudhury, B.U. Nair, R. Ghosh, Polyhedron. 107 (2016) 1-8.
[53] T. Ghosh, J. Adhikary, P. Chakraborty, P.K. Sukul, M.S. Jana, T.K. Mondal, E. Zangrando, D. Das, Dalton Trans. 43 (2014) 841-852.
[54] M.J. Goldcamp, D.M. Goldcamp, K. Slack, M.J. Baldwin, Inorg. Chem. Commun. 63 (2016) 53-56.
[55] S. Mistri, H. Puschmann, S.C. Manna, Polyhedron. 115 (2016) 155-163.

[56] R. Modak, Y. Sikdar, S. Mandal, S. Chatterjee, A. Bienko, J. Mrozinski, S. Goswami, Inorg. Chim. Acta. 416 (2014) 122-134.
[57] S. Mondal, B. Pakhira, A.J. Blake, M.G.B. Drew, S.K. Chattopadhyay, Polyhedron. 117 (2016) 327-337.
[58] A. Pal, S.C. Kumar, A.K. Ghosh, C. Lin, E. Riviere, T. Mallah, R. Ghosh, Synthesis, Polyhedron. 110 (2016) 221-226.
[59] S. Roy, S.K. Sarkar, R. Saha, T.K. Mondal, C. Sinha, Inorg. Chim. Acta. 482 (2018) 659-668.
[60] K. Serbest, O. Goktekin, K. Karaoglu, A. Zengin, U. Coruh, Heteroat. Chem. 29 (2018) e21439.
[61] K. Das, T.K. Mondal, E. Garribba, M. Fondo, C. Sinha, A. Datta, Inorg. Chim. Acta. 413 (2014) 194-202.
[62] A. Guha, T. Chattopadhyay, N.D. Paul, M. Mukherjee, S. Goswami, T.K. Mondal, E. Zangrando, D. Das, Inorg. Chem. 51 (2012) 8750-8759.
[63] S.K. Mal, M. Mitra, C.S. Purohit, R. Ghosh, Polyhedron. 101 (2015) 191-195.
[64] A. Patra, G.C. Giri, T.K. Sen, L. Carrella, S.K. Mandal, M. Bera, Polyhedron. 67 (2014) 495-504.
[65] R. Sanyal, S.K. Dash, S. Das, S. Chattopadhyay, S. Roy, D. Das, J. Biol. Inorg. Chem. 19 (2014) 1099-1111.
[66] L. Simandi, T. Simandi, J. Chem. Soc., Dalton Trans. (1998) 3275-3279.
[67] T. Simandi, L. Simandi, Reac. Kinet. Catal. L. 65 (1998) 301-309.
[68] J. Qiu, Z. Liao, X. Meng, L. Zhu, Z. Wang, K. Yu, Polyhedron. 24 (2005) 1617-1623.
[69] A. Banerjee, A. Guha, J. Adhikary, A. Khan, K. Manna, S. Dey, E. Zangrando, D. Das, Polyhedron. 60 (2013) 102-109.
[70] R. Modak, Y. Sikdar, S. Mandal, S. Goswami, Inorg. Chem. Commun. 37 (2013) 193-196.
[71] S.K. Dey, A. Mukherjee, New J. Chem. 38 (2014) 4985-4995.
[72] A. Hazari, L.K. Das, R.M. Kadam, A. Bauza, A. Frontera, A. Ghosh, Dalton Trans. 44 (2015) 3862-3876.
[73] R.M. Buchanan, C.G. Pierpont, J. Am. Chem. Soc. 102 (1980) 4951-4957.
[74] P. Hormnirun, E.L. Marshall, V.C. Gibson, R.I. Pugh, A.J.P. White, Proc. Natl. Acad. Sci. U. S. A. 103 (2006) 15343-15348.
[75] SMART and SAINT, Area Detector Software Package and SAX Area Detector Integration Program, Bruker Analytical X-ray, Madison, WI, USA, 1997.
[76] SADABS, Area Detector Absorption Correction Program, Bruker Analytical X-ray, Madison, WI, USA, 1997.
[77] G.M. Sheldrick, Acta Cryst. A. 64 (2008) 112-122.
[78] S. Stoll, A. Schweiger, J. Magn. Reson. 178 (2006) 42-55.
[79] H. Furutachi, H. Okawa, Inorg. Chem. 36 (1997) 3911-3918.
[80] L. Rodriguez, E. Labisbal, A. Sousa-Pedrares, J.A. Garcia-Vazquez, J. Romero, M.L. Duran, J.A. Real, A. Sousa, Inorg. Chem. 45 (2006) 7903-7914.
[81] S. Kita, H. Furutachi, H. Okawa, Inorg. Chem. 38 (1999) 4038-4045.
[82] M. Du, D. An, Y. Guo, X. Bu, J. Mol. Struct. 641 (2002) 193-198.
[83] A.W. Addison, T.N. Rao, J. Reedijk, J. van Rijn, G.C. Verschoor, J. Chem. Soc., Dalton Trans. (1984) 1349-1356.
[84] R. Boca, H. Elias, W. Haase, M. Huber, R. Klement, L. Muller, H. Paulus, I. Svoboda, M. Valko, Inorg. Chim. Acta. 278 (1998) 127-135.
[85] J. Balla, T. Kiss, R. Jameson, Inorg. Chem. 31 (1992) 58-62.
[86] J. Manzur, A. Garcia, V. Rivas, A. Atria, J. Valenzuela, E. Spodine, Polyhedron. 16 (1997) 2299-2305.
[87] J. Manzur, A. Garcia, B. Gomez, E. Spodine, Polyhedron. 19 (2000) 2367-2372.
[88] H. Tadokoro, S. Nishiyama, S. Tsuruya, M. Masai, J. Catal. 138 (1992) 24-37.
[89] M. Tumer, D. Ekinci, F. Tumer, A. Bulut, Spectrochim. Acta A. 67 (2007) 916-929.
[90] P. Chakraborty, S. Mohanta, Inorg. Chim. Acta. 435 (2015) 38-45.
[91] O. Kahn, Angew. Chem. Int. Ed. Engl. 24 (1985) 834-850.
[92] S. Thamban, U. Arjun, M. Padmanabhan, R. Nath, J. Phys. -Condes. Matter. 29 (2017) 255801.
[93] J. Faus, M. Julve, F. Lloret, M. Munoz, Inorg. Chem. 32 (1993) 2013-2017.
[94] C. Ohrenberg, P. Ge, P. Schebler, C. Riordan, G. Yap, A. Rheingold, Inorg. Chem. 35 (1996) 749-754.

[95] A. Ozarowski, H. Lee, A. Balch, J. Am. Chem. Soc. 125 (2003) 12606-12614.
[96] B. Santra, G. Lahiri, J. Chem. Soc., Dalton Trans. (1998) 139-145.
[97] A. Sengupta, A. Rajput, S.K. Barman, R. Mukherjee, Dalton Trans. 46 (2017) 11291-11305.
[98] M. Symons, T. Taiwo, A. Sargeson, M. Ali, A. Tabl, Inorg. Chim. Acta. 241 (1996) 5-8.
[99] M. Xu, Z. Liu, B. Dong, H. Cui, Y. Wang, J. Su, Z. Wang, Y. Song, X. Chen, S. Jiang, S. Gao, Inorg. Chem. 58 (2019) 2330-2335.
[100] S. Arzberger, J. Soper, O. Anderson, A. la Cour, M. Wicholas, Inorg. Chem. 38 (1999) 757-761.
[101] M. Brown, B. McGarvey, A. Ozarowski, D. Tuck, J. Am. Chem. Soc. 118 (1996) 9691-9694.
[102] S. Majumder, S. Mondal, P. Lemoine, S. Mohanta, Dalton Trans. 42 (2013) 4561-4569.
[103] A. Das, K. Bhattacharya, L.K. Das, S. Giri, A. Ghosh, Dalton Trans. 47 (2018) 9385-9399.
[104] D. Adams, A. Dei, A. Rheingold, D. Hendrickson, J. Am. Chem. Soc. 115 (1993) 8221-8229.
[105] D. Adams, L. Noodleman, D. Hendrickson, Inorg. Chem. 36 (1997) 3966-3984.
[106] E. Evangelio, D. Ruiz-Molina, Eur. J. Inorg. Chem. (2005) 2957-2971.
[107] C. Roux, D. Adams, J. Itie, A. Polian, D. Hendrickson, M. Verdaguer, Inorg. Chem. 35 (1996) 2846-2852.

Author statement

Shuranjan Sarkar : Methodology, Validation, Formal analysis, Investigation, Data curation, Writing - Original Draft, Visualization,

Hong-In Lee : Conceptualization, Software, Resources, Data Curation, Writing - Review & Editing, Visualization, Supervision, Project administration, Funding acquisition,

Declaration of interests

☒ The authors declare that they have no known competing financial interests or personal relationships that could have appeared to influence the work reported in this paper.

☐The authors declare the following financial interests/personal relationships which may be considered as potential competing interests:

Graphical Abstract

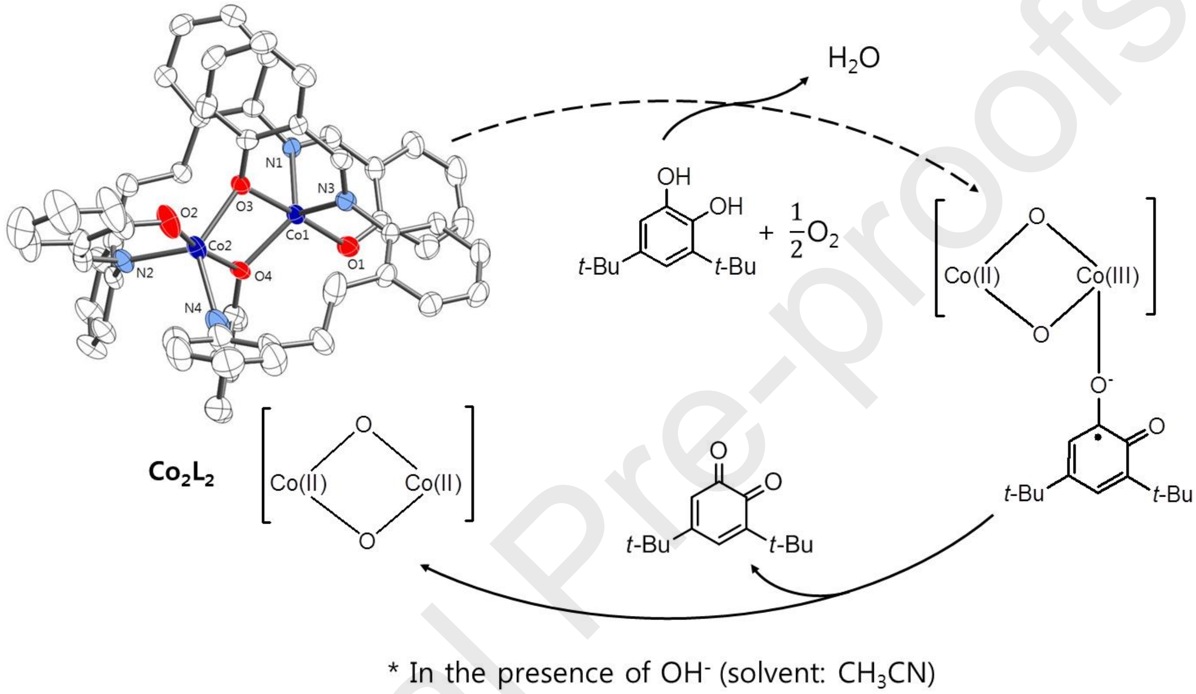

Highlights

- A dinuclear cobalt complex (Co_2L_2) derived from a tetradentate diphenolate ligand H_2L (H_2L = *N,N'*-bis(salicylidene)-2,2'-ethylenedianiline) was synthesized.
- Single crystal X-ray crystallography revealed that Co_2L_2 is a dimeric complex with a planar $Co(II)_2O_2$ core.
- Magnetic susceptibility measurements on Co_2L_2 found that both Co(II) ions are in low-spin (S = 1/2) states and two Co(II) spin centers are antiferromagnetically coupled.
- The complex showed a high catecholase activity when it reacted with 3,5-di-*tert*-butylcatechol (3,5-H_2dtbc) in the presence of O_2 and NaOH.
- Electron paramagnetic resonance (EPR) of the catalytic reaction mixture observed a key reaction intermediates, 3,5-di-*tert*-butyl-1,2-benzosemiquinonate anion radical (3,5-dtsq$^{\bullet -}$) bound to Co(III)-center.